Structural Characterization of the Redox Behavior in Copper-Exchanged Sodium Zeolite Y by High-Resolution Powder Neutron Diffraction

A. J. Fowkes,[†] R. M. Ibberson,*[,‡] and M. J. Rosseinsky*[,§]

Inorganic Chemistry Laboratory, Department of Chemistry, University of Oxford, South Parks Road, Oxford OX1 3QR, U.K., ISIS Facility, CLRC−Rutherford Appleton Laboratory, Chilton, Didcot, OXON OX11 0QX, U.K., and Department of Chemistry, University of Liverpool, Liverpool L69 7ZD, U.K.

Received May 21, 2001. Revised Manuscript Received October 22, 2001

The results of structural refinements on high-resolution powder neutron diffraction data for copper(II)- and copper(I)-exchanged zeolite Y and for the parent sodium zeolite Y, with composition $Na_{62}Si_{128}Al_{64}O_{384}$, are presented. Rietveld refinement of ambient-temperature data shows that the Cu(I) and Cu(II) cations are located on different sites in the two materials and that the structures differ considerably from that adopted by NaY. In $Cu^{II}Y$, with composition $Cu_{33}Na_{12}Si_{130}Al_{62}O_{384}$, the copper cations are located on the I_A', I_B', and II′ sites with occupancies of 0.552(4), 0.145(7), and 0.162(8), respectively, while some sodium, 0.36-(2), remains on site II. For $Cu^{I}Y$, there is a redistribution of the cations on sites I_A', I_B', II′, and II to 0.39(2), 0.21(1), 0.24(1), and 0.18(2), respectively. In both zeolites, site I is vacant. The high-quality diffraction data provide direct evidence of structural changes associated with the redox behavior of the zeolite, including distortion of the framework and the location of charge-balancing species.

Introduction

There is considerable current interest in the ion exchange of copper into zeolites.[1−5] The focus of studies in this area is the catalytic activity of the materials, in particular their ability to remove nitric oxide from automobile exhaust streams, by the selective binding and catalytic reduction of NO. In 1978, the first reports of the catalytic behavior of copper-exchanged zeolite Y ($Cu^{II}Y$) for this process were published by Kagawa et al.[6] The copper-exchanged zeolites ZSM-5[7] and mordenite[8] show yet higher catalytic activity than the Y-type copper-exchanged zeolite. Turnover frequencies per copper cation are 28.8×10^3, 0.74×10^3, and 0.17×10^3 for Cu−ZSM-5, copper mordenite, and CuY, respectively.[9] High levels of copper exchange produce large increases in catalytic behavior for a given zeolite.[9] Reduction of $Cu^{II}Y$ in 4% CO in He for 2 h increases the catalytic activity, indicating the importance of the Cu oxidation state.[9] The accurate determination of the crystal structures of Cu(I)- and Cu(II)-exchanged zeolite Y is therefore an important step in understanding the chemistry of copper-exchanged zeolites, as Si/Al ratios higher than those found in ZSM-5 permit the accurate location of extraframework cations in both oxidized and reduced forms.

Zeolite Y is a synthetic form of the mineral faujasite. The crystal structure, illustrated in Figure 1, consists of a sodium aluminosilicate framework with a Si/Al ratio varying between 1.5 and 3.0. In zeolite Y, the number of aluminum ions in the unit cell varies according to the relation between the number of tetrahedral Al atoms, N_{Al}, and the Si/Al ratio such that

$$N_{Al} = \frac{192}{(1 + R)}$$

where $R = N_{Si}/N_{Al}$. In zeolite Y, N_{Al} is typically in the range between 76 and 48. The framework structure can be described as a diamond array of cuboctahedral aluminosilicate units composed of 24 (Si, Al) atoms and 36 oxygen atoms. Each unit cell consists of 8 large absorption cages with a 13.7-Å free diameter (the supercages), 8 sodalite units (the main structural units), and 16 hexagonal prisms. Channels of 7.5-Å diameter form where the supercages meet.

A number of possible sites within the framework are available for the location of the cations required to balance the charge on the aluminosilicate framework (see Figure 1). Site I is located at the center of the

* To whom correspondence should be addressed. E-mail: m.j.rosseinsky@liv.ac.uk, rmi@isise.rl.ac.uk.
[†] University of Oxford.
[‡] CLRC−Rutherford Appleton Laboratory.
[§] University of Liverpool.

(1) Attfield, M. P.; Weigel, S. J.; Cheetham, A. K. *J. Catal.* **1997**, *172*, 274−280.
(2) Attfield, M. P.; Weigel, S. J.; Cheetham, A. K. *J. Catal.* **1997**, *170*, 227−235.
(3) Nachtigallova, D.; Nachtigall, P.; Sauer, J. *Phys. Chem. Chem. Phys.* **2001**, *3*, 1552−1559.
(4) Schay, Z.; James, V. S.; Pal-Borbely, G.; Beck, A.; Ramaswamy, A. V.; Guczi, L. *J. Mol. Catal. A: Chem.* **2000**, *162*, 191−198.
(5) Palomino, G. T.; Bordiga, S.; Zecchina, A.; Marra, G. L.; Lamberti, C. *J. Phys. Chem. B* **2000**, *104*, 8641−8651.
(6) Kagawa, S.; Yokoo, S.; Iwamoto, M. *J. Chem. Soc., Chem. Commun.* **1978**, 1058−1059.
(7) Iwamoto, M.; Furukawa, H.; Kagawa, S. *New Developments in Zeolites, Science and Technology*; Elsevier: Amsterdam, 1986.
(8) Shelef, M. *Chem. Rev.* **1995**, *95*, 209−225.
(9) Li, Y.; Hall, W. K. *J. Catal.* **1991**, *129*, 202−215.

10.1021/cm010504b CCC: $22.00
Published on Web 01/18/2002

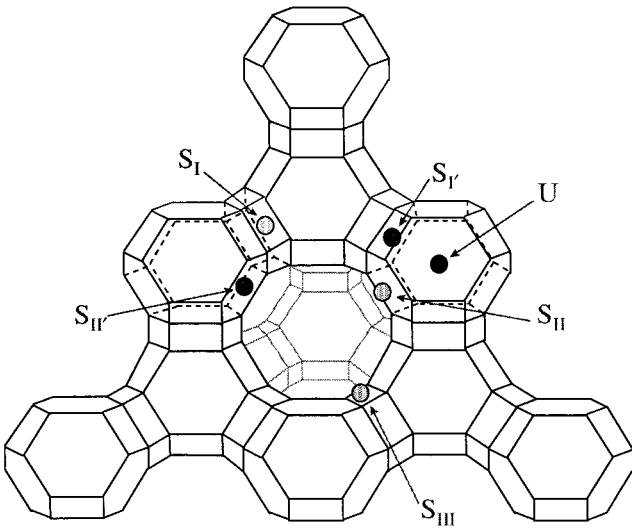

Figure 1. Schematic diagram of the structure of zeolite Y, faujasite, showing locations of the cation sites.

hexagonal prism and is octahedrally coordinated to the framework. Site II is on the six-membered-ring face of the sodalite cage on the supercage side and has three nearest neighbors. Sites I′ and II′ lie on the other sides of the six-membered rings, opposite sites I and II, respectively, inside the sodalite cage and are also 3-fold-coordinate. Site III is occupied for some zeolites and is located at the center of the square faces of the sodalite unit.

Ion exchange is dependent on a number of factors such as cation size and oxidation state, level of hydration of the zeolite, and silicon/aluminum ratio of the framework.[10] These factors determine the location of the cations and also the possible extent and kinetics of exchange. Sites I, I′, and II are occupied for the majority of the alkali-metal- and alkaline-earth-metal-exchanged NaY samples.[11−13] In Na-exchanged Y with a Si/Al ratio of 2.43, cations are located at the I, I′, and II sites, the latter being fully occupied.[14] The cation distribution can be further modified by adsorption of water,[15] and additional sites, at much greater distances from the framework because of cation bonding with sorbed water, can also be occupied. For NaY itself, in the presence of an equilibrium water pressure, the I′ occupancy increases, but neither the site I nor the site II populations reach the level of occupancies of the dehydrated state, and it is impossible to locate crystallographically all of the analytically determined cations.[16]

CuY can be reversibly reduced and reoxidized. A key issue raised by this property, which is central to the catalytic activity of Cu-exchanged zeolites, is the charge balance of the framework.[17−21] The extraframework cations balance the negative charge arising as a result of the substitution of aluminum ions for silicon. If, during ion exchange, two sodium cations are replaced with one Cu^{2+} cation, then, upon reduction of the copper from the divalent to the monovalent state, assuming no other changes, residual negative charge equal to the number of copper cations reduced is left on the framework. Two possible explanations for this behavior have been proposed. The first postulates that, upon reduction of the cation, oxygen is removed from the framework, leading to a dealumination of the framework according to eq 1[18]

$$2Cu^{2+} + (AlO_2)_{fw}^{-} + CO \rightarrow CO_2 + (AlO)_{efw}^{+} + 2Cu^{+} \quad (1)$$

There is diffraction-based precedent for extraframework aluminum in other, non-Cu zeolites.[22] Neutron powder diffraction[23] shows that dealumination of H-zeolite Y yields AlO_4 units at the center of the sodalite cage, although the protons or deuterons expected to be bound to the framework or the AlO_4 unit can not be located because of their positional disorder. This extraction of Al^{3+} from the framework might be expected to lead to vacancies on the T site, but X-ray powder diffraction studies on 53% dealuminated (Na, H)Y (84% expected T-site occupancy)[24] indicate that the T-site occupancy remains at 1. This shows that dealumination occurs by local recrystallization of the framework by the formation of new SiO_4 tetrahedra in regions of the framework damaged by alumina removal.

^{29}Si and ^{27}Al MAS NMR experiments on CuY reduced with H_2 and CO[20] show that the maximum extent of dealumination is 35% of that required by the scheme proposed in ref 18. From this finding, it was deduced that extraframework oxygen (EFO) must have been introduced into the zeolite during preparation to allow the reversible redox behavior, e.g.

$$2Cu^{II}OH^{+} + CO(g) \rightarrow 2Cu^{I} + CO_2(g) + H_2O(g) \quad (2)$$

The mechanism of introduction of EFO into $Cu^{II}Y$ must differ from that in zeolites containing oxidizable cations: EFO can be introduced into $Fe^{II}Y$ without overexchange by subsequent oxidation to $Fe^{III}Y$,[25] but in the CuY case, the Cu^{II} cations introduced by ion exchange need to be reduced, before reoxidation with the introduction of EFO is possible.

The introduction of extraframework oxygen is closely related to overexchange of divalent Cu^{2+} cations for Na^{+} in the preparation of Cu-loaded zeolites and to the ability of the zeolite to act as an oxygen carrier in catalytic reactions. The $Cu(OH)^{+}$ unit shown in eq 2

(10) Barry, T. I.; Lay, L. A. *J. Phys. Chem. Solids* **1968**, *29*, 1395−1405.
(11) Dun, J. J. I. V.; Mortier, W. J.; Uytterhoeven, J. B. *Zeolites* **1985**, *5*, 257−260.
(12) Breck, D. W. *Zeolite Molecular Sieves*: *Structure, Chemistry and Use*; R. E. Krieger: Malabar, FL, 1984.
(13) Herden, H.; Einicke, W. D.; Schollner, R.; Mortier, W. J.; Gellens, L. R.; Uytterhoeven, J. B. *Zeolites* **1982**, *2*, 131−134.
(14) Fitch, A. N.; Jobic, H.; Renouprez, A. *J. Phys. Chem.* **1986**, *90*, 1311−1318.
(15) Mortier, W. J. *Compilation of Extra Framework Sites in Zeolites*; Butterworth Scientific Ltd.: Oxford, U.K., 1982.
(16) Mortier, W. J.; Bossche, E. V. D.; Uytterhoeven, J. B. *Zeolites* **1984**, *4*, 41−44.
(17) Naccache, C. M.; Ben Taarit, Y. *J. Catal.* **1971**, *22*, 171−181.
(18) Jacobs, P. A.; Beyer, H. K. *J. Phys. Chem.* **1979**, *83*, 1174−1177.
(19) Petunchi, J. O.; Hall, W. K. *J. Catal.* **1983**, *80*, 403−418.
(20) Petunchi, J. O.; Marcelin, G.; Hall, W. K. *J. Phys. Chem.* **1992**, *96*, 9967−9975.
(21) Valyon, J.; Hall, W. K. *J. Phys. Chem.* **1993**, *97*, 7054−7060.
(22) Nery, J.; Mascarenhas, Y. P.; Bonagamba, T. J.; Mello, N. C.; Souza-Aguiar, E. F. *Zeolites* **1997**, *18*, 44−49.
(23) Parise, J. D.; Corbin, D. R.; Abrams, L. *Acta Cryst. C* **1984**, *40*, 1493.
(24) Gallezot, P.; Beaumont, R.; Barthomeuf, D. *J. Phys. Chem.* **1974**, *78*, 1550.
(25) Garten, R. L.; Delgass, W. N.; Boudart, M. *J. Catal.* **1970**, *18*, 90.

represents a variety of lower-charged cationic species, such as $Cu_2(OH)_2^{2+}$,[26,27] present in Cu(II) solutions as a result of hydrolysis [to form $Cu(OH)^+$] and subsequent condensation increasingly favored with higher pH. These species can be introduced into the zeolite by exchange for Na^+. Alternatively, $[CuOH]^+$ can be generated upon dehydration of the zeolite. These processes lead to the introduction of an excess of Cu cations over the amount expected for a Cu(II)/2Na^+ exchange. Overexchange (of up to 600%) is common in ion-exchanged ZSM-5 samples and has been observed in mordenites:[28] it is enhanced above pH 6.[29] The maintenance of charge balance in the Cu(II)-exchanged zeolite is achieved by the incorporation of extraframework anionic ligands such as oxide or hydroxide. Overexchange has been observed in zeolite Y[30] exchanged with 0.1 M copper chloride. IR spectroscopy showed that hydroxyl groups (assigned to $[CuOH]^+$) are present in the overexchanged samples. The analytical data indicate that these hydroxyl groups originate from the ion-exchange procedure and not from the dissociation of water molecules. The catalytic activity of the zeolite to oxidation of CO increases with the extent of Cu overexchange.[9] There is EPR[31] and TPD[32] evidence for EFO in $Cu^{II}Y$, assigned without structural evidence to oxygen bridging two Cu(I′) sites.

The literature on the crystal structure of $Cu^{II}Y$ is restricted, and to our knowledge, no reports exist on the structure and location of cations in $Cu^{I}Y$ prepared by reduction of $Cu^{II}Y$. The room-temperature structures of hydrated and dehydrated divalent-copper-exchanged faujasite were determined by Maxwell and de Boer using single-crystal X-ray diffraction with Cu radiation on ion-exchanged crystals of natural faujasite (with potassium ions and subsequently with Cu^{2+}). The Si/Al ratio was estimated from the unit cell constant as Si/Al = 2.42, close to the accepted value for natural faujasite reported by Baur.[33] Close to 100% exchange of copper for potassium was assumed, and overexchange of cations was not considered. These refinements indicated that copper is located on the site I′ in the hydrated form and that copper cations are located on the sites I, I′, II′, II, and III in the dehydrated form (dehydrated at 150 °C for 20 h at 10^{-5} Torr). However, although credible overall, some details of the refined structures are less than compelling, and satisfactory refinement required exclusion of the (111) reflection. For example, the refined isotropic temperature factors for some of the cation sites are especially large (in some cases over 10 Å^2), and the accompanying site occupancy factors very small, leading to some doubt as to the precise structure of the dehydrated zeolite. Gallezot et al.[34] had earlier used X-ray powder diffraction on the dehydrated copper-exchanged zeolites $Cu_{16}Na_{24}Y$ and $Cu_{12}Na_5H_{27}Y$ to locate copper cations on the I and I′ sites and Na on the II site. Marti et al. found copper cations on the II and III sites in the supercage in a number of hydrated zeolite Y samples with varying sodium/copper ratios.[35] It was deduced that sodium cations occupied site I, as the occupancy of this site decreased as the copper content of the samples increased. A recent study of solid-state-exchanged $Cu^{II}Y$ containing entrained $CuCl_2$ finds that the I, I′, and III′ (slightly displaced from III) sites are occupied.[36]

This paper describes the determination of the structures of $Cu^{II}Y$ and $Cu^{I}Y$ from high-resolution powder neutron diffraction data. A key point of the present study is the use of diffraction methods to establish the structure of $Cu^{I}Y$ and to address the issue of T-site occupancy and the extent of dealumination via the ratio of the T to extraframework sites. The high-quality diffraction data enable structural changes associated with the redox behavior of the zeolite, including distortion of the framework and location of charge-balancing species as postulated above, to be characterized. Evidence for framework dealumination and significant rearrangement of the extraframework cations upon reduction is provided.

Experimental Section

(1) Preparation of NaY. NaY was supplied by Unilever. The zeolite was first washed with aqueous $NaNO_3$ solution to remove cation vacancies and to ensure that all cations are present as Na^+, not H^+.[37] After filtration, the substrate was washed with deionized water to remove $NaNO_3$ and then dried at 373 K in a drying oven. The zeolite was stored over a saturated solution of NH_4Cl in a desiccator before it was ion exchanged. For neutron diffraction measurements, a sample devoid of water was required, so the sample was vigorously degassed. The zeolite was placed in alumina boats in a gas flow tube in a furnace. Oxygen gas was continually flowed over the sample while it was heated at 1 ° min^{-1} to 373 K. The temperature was held for 4 h to drive off the water before being increased at a rate of 1 ° min^{-1} to 673 K, where it was left for 4 h. The sample was cooled to room temperature and transferred to an M. Braun Labmaster drybox, where it was stored under helium. The pretreated zeolite was subsequently loaded into a silica ampule, sealed with a Young's tap, and then removed to a vacuum line where it was degassed under vacuum (10^{-5} Torr) in a furnace at 673 K for 4 h. The sample was cooled to room temperature under vacuum and removed to the drybox where it was stored.

(2) Preparation of $Cu^{II}Y$. Ten grams of NaY, previously washed with $NaNO_3$, was stirred for 48 h in 1 L of 1.0 M $CuCl_2$ (BDH, Analar, 99.9%) in D_2O (Fluorochem, 99.9% D) solution. This is analogous to the procedure described by Schoonheydt et al.[30] The zeolite was washed several times with D_2O to remove the excess copper chloride. The solid produced was blue-green colored.

At this stage, the sample can contain surface defects and also a large amount of residual water. The level of hydration of the zeolite strongly influences the siting of the cations. When water is bound to the copper cations, it often results in migration of $Cu(OH_2)_6^{2+}$ to the supercages, making cation location by diffraction methods almost impossible.[38] For our experiments, samples as fully dehydrated as possible were

(26) Stumm, W.; Morgan, J. J. *Aquatic Chemistry*: *An Introduction Emphasising Chemical Equilibria in Natural Waters*; Wiley: New York, 1981.
(27) Pass, G. *Ions in Solution (3)*; Clarendon Press: Oxford, U.K., 1973.
(28) Kuroda, Y.; Kotami, A.; Maeda, H.; Morimoto, H. *J. Chem. Soc., Chem. Commun.* **1989**, 1631.
(29) Valyon, J.; Hall, W. K. *Catal. Lett.* **1993**, *19*, 109−119.
(30) Schoonheydt, R. A.; Vandamme, L. J.; Jacobs, P. A.; Uytterhoeven, J. B. *J. Catal.* **1976**, *43*, 292−303.
(31) Chao, C. C.; Lunsford, J. H. *J. Chem. Phys.* **1972**, *57*, 2890.
(32) Iwamoto, M.; Nakamura, M.; Nagano, H.; Kagawa, S.; Selyama, T. *J. Phys. Chem.* **1982**, *86*, 153−156.
(33) Baur, W. H. *Am. Miner.* **1964**, *49*, 697.
(34) Gallezot, P.; Ben Taarit, Y.; Imelik, B. *J. Catal.* **1972**, *26*, 295−302.
(35) Marti, J.; Soria, J.; Cano, F. H. *J. Phys. Chem.* **1976**, *80*, 1776.
(36) Haniffa, R. M.; Seff, K. *Microporous Mesoporous Mater.* **1998**, *25*, 137−149.
(37) Jacobs, P. A.; Tielen, M.; Linart, J. P.; Uytterhoeven, J. B.; Beyer, H. *J. Chem. Soc., Faraday Trans. 1* **1976**, *72*, 2793.

required. The sample was pretreated in oxygen, as described for the NaY sample above, and vigorously degassed under vacuum at 400 °C by the same procedure as for NaY. The sample was still blue at this point but somewhat paler (this is attributed to loss of water). It is possible that some of the copper has been reduced by this procedure to Cu^+, although a strong EPR signal can still be observed. Petunchi and Hall observed about 10% reduction of Cu^{2+} to Cu^+ on evacuation at the higher temperature of 500 °C.[19]

(3) Preparation of $Cu^{I}Y$. Five grams of the $Cu^{II}Y$ sample, prepared by ion exchange and pretreated with oxygen at 673 K, was loaded into an 18-mm quartz insert and placed in a silica gas flow tube. The tube was placed in a furnace, evacuated, and then heated slowly to 753 K. Carbon monoxide gas at 1 bar pressure was passed over the zeolite and then through a paraffin oil bubbler for 2−3 min. The sample was left for 30 min under static CO pressure, and then once again CO was passed over the zeolite. After an additional 30 min, the gas flow tube was evacuated at 10^{-3} Torr and then cooled to room temperature. The $Cu^{I}Y$ sample obtained was white. Complete reduction from Cu(II) to Cu(I) was confirmed by the absence of a signal in the EPR spectrum.

(4) Chemical Analysis. Chemical analysis was used to determine the approximate compositions of NaY and $Cu^{II}NaY$ in terms of the cations present by Analytische Laboratorien. A fully hydrated sample of the zeolite was dissolved using HF in a sealed PTFE vessel at 373 K. The HF was complexed with boric acid prior to dilution and analysis. For Cu, Si, and Al, analysis was carried out using the atomic absorption flame technique, and for Na, flame photometry was used. This analysis showed the composition of the parent zeolite to be $Na_{62}H_2Si_{128}Al_{64}O_{384}\cdot 252H_2O$ and that of the copper-exchanged zeolite to be $Cu_{33}Na_{12}Si_{130}Al_{62}O_{384}\cdot 185H_2O$. NaY (%): Na, 8.18 calc (8.18 obs); Al, 9.91 (9.90); Si, 20.62 (20.65). CuNaY (%): Na 1.61 (1.61); Cu, 12.21 (12.25); Al, 9.74 (9.74); Si, 21.3 (21.2).

The analytical data indicate an overexchange of 7 Cu^{II} cations per formula unit given the exchange of 50 Na^+ and 2 H^+ ions per formula unit, consistent with the data of Schoonheydt et al. for CuY zeolites exchanged under the same conditions.[30] EDX data indicated no excess chloride incorporated into the samples, excluding the possibility of entrained $CuCl_2$ contamination as the source of the analytical copper excess. Cu oxidation states were not determined directly.

(5) X-ray Powder Diffraction Measurements. The benefit of joint X-ray and neutron refinements in overcoming the difficulties associated with each in the initial assignment of cations and the subsequent refinement of their site occupancies is well-known.[39] With this in mind, X-ray data were collected on a Siemens D5000 diffractometer operating in transmission mode with a 6° linear-position-sensitive detector. Cu $K\alpha_1$ radiation (40 kV, 30 mA) with a wavelength of 1.54056 Å was used. Zeolite samples were loaded in 0.7-mm capillaries in a helium drybox and sealed. Data were collected initially for 1 h over the angular range 5−40 ° to confirm the sample purity. A 2-day dataset was subsequently recorded for multisource Rietveld refinement together with the neutron data. However, problems were soon recognized because of radiation damage to the zeolite samples. A comparison of data collected on the same capillary of $Cu^{II}Y$ after 1-h and 2-day data collections revealed marked differences between the diffraction patterns. The relative intensities of a number of reflections had changed. The same behavior was observed for $Cu^{I}Y$: the color of these samples changed from white to pale blue during irradiation.

(6) Neutron Powder Diffraction Measurements. For the neutron diffraction experiments, 4-g samples of dehydrated $Cu^{II}Y$, $Cu^{I}Y$, and NaY were loaded under helium in the drybox into 15-mm-diameter, electron-beam-welded, cylindrical vanadium cans, which were then sealed using indium wire. Diffraction data were collected at 298 K for the copper-exchanged zeolites and NaY. Experiments were carried out on the HRPD (high-resolution powder diffractometer) at ISIS at the Rutherford Appleton Laboratory. Data were typically collected for 350 μA (ca. 8−10 h) on each CuY sample over the *d*-spacing range 0.83−10.0 Å and for 280 μA (ca. 16 h) for NaY over an extended *d*-spacing range up to 15 Å.

Data from the main backscattering (168°) detector bank of HRPD plus 90° and low-angle (30°) data were normalized and refined by the Rietveld method using GSAS software.[40] The relevant coherent neutron scattering lengths are Si, 4.15; Al, 3.45; O, 5.81; Na, 3.63; and Cu, 7.72 fm. A shifted Chebyshev background function was used for all refinements. The peak shape was described in terms of one Lorentzian and one Gaussian function only.

Structure Determination

Data from all three banks on HRPD were refined in the space group $Fd\bar{3}m$. In the final refinement cycles, the lattice parameter, background, profile parameters, and atomic temperature factors and positional parameters were refined. The copper cation fractional site occupancies could be refined without constraint in all cases. The temperature factors for the extraframework cations were refined as isotropic and were constrained to be the same for all cations within each refinement. The silicon and aluminum site fractional occupancies were fixed at the values determined by the chemical analysis. Small peaks due to vanadium from the sample were excluded from the refinements. Table 1 lists the refined positional parameters with their estimated standard deviations (esd's) for the three samples. Table 2 contains the bond lengths and angles for the framework as refined at 298 K. Tables 3 and 4 give refined cation-related interatomic distances and angles, and Table 5 shows the refinement statistics.

(1) NaY. The refinement of the NaY starting material is comparable with the results of Fitch et al.,[14] indicating the absence of dealumination in the initial zeolite. The refined parameters are given in Table 1. The refined stoichiometry is $Na_{51(1)}Si_{128}Al_{64}O_{384}$, with the unlocated sodium probably occupying sites in the supercages. The II, I, and I′ sites are all occupied, with the II site being 100(1)% full. Tables 2 and 6 give the T−O and Na−O distances in NaY. The Rietveld fit is given in the Supporting Information.

(2) $Cu^{II}Y$. The structural refinement of the copper-exchanged zeolites proved complicated, and we report a detailed description of the characterization of the structures here. Errors in the model might mask subtle structural details, and this fact proved to be a problem in locating the small number of extraframework species with limited contributions to the intensities of the Bragg reflections.

Initial refinements used the model of Maxwell and de Boer[38] for dehydrated divalent-copper-exchanged faujasite. This sample differs in its preparation and stoichiometry from the $Cu^{II}Y$ material in this study. The fit was poor ($\chi^2 = 7.679$) and attempts to refine the cation positions resulted in divergence of the refinement. The sodium and framework positions from the model refined for NaY were therefore used as a starting point. The positions of framework atoms were refined initially. The fit was poor at this stage, indicating the extent of the contribution of the copper cations to the diffraction

(38) Maxwell, I. E.; de Boer, J. J. *J. Phys. Chem.* **1975**, *79*, 1874−1879.

(39) Cheetham, A. K.; Wilkinson, A. P. *J. Phys. Chem. Solids* **1991**, *52*, 1199−1208.

(40) Larsen, A.; Von Dreele, R. B. *The General Structure Analysis System*; Los Alamos National Laboratory: Los Alamos, NM, 1985.

Table 1. Refined Positional Parameters with Estimated Standard Deviations for NaY, $Cu^{II}Y$, and $Cu^{I}Y$ at 298 K[a]

		NaY	$Cu^{II}Y$	$Cu^{I}Y$
Si/Al	*x*	0.03571(11)	0.03635(11)	0.0365(1)
	y	0.30458(9)	0.30270(10)	0.3036(1)
	z	0.12499(10)	0.12459(10)	0.1244(1)
	U	0.017*	0.028*	0.014*
O(1)	*x*	0	0	0
	y = −*z*	−0.10637(8)	−0.10353(13)	−0.1045(1)
	U	0.025*	0.052*	0.038*
O(2)	*x* = *z*	0.00268(7)	0.00197(10)	0.0023(1)
	y	−0.14213(10)	−0.14144(16)	−0.1432(1)
	U	0.026*	0.088*	0.040*
O(3)	*x* = *z*	0.07317(8)	0.07356(9)	0.0752(1)
	y	−0.03358(11)	−0.02789(13)	−0.0305(2)
	U	0.031*	0.067*	0.041*
O(4)	*x* = *z*	0.07200(10)	0.07342(10)	0.0728(1)
	y	0.31746(12)	0.32050(15)	0.3227(1)
	U	0.034*	0.061*	0.039*
O(20)	*x*	–	0.1462(18)	0.1388(4)
EFO	*y* = *z*	–	0.1116(10)	0.1388(4)
	frac	–	0.047(1)	0.145(5)
	P	–	4.51(9)	4.6(2)
	U	–	0.073(4)	0.072(5)
D(21)	*x*	–	0.1462(18)	0.1388(4)
	y = *z*	–	0.1116(10)	0.1388(4)
	frac	–	0.047(1)	0.145(5)
	P	–	4.51(9)	4.6(2)
	U	–	0.073(4)	0.072(5)
I	*x* = *y* = *z*	0	–	–
	cation	Na	–	–
	frac	0.631(18)	–	–
	P	10.10(30)	–	–
I_A'	*x* = *y* = *z*	0.0540(4)	0.05015(20)	0.0549(8)
	cation	Na	Cu	Cu
	frac	0.285(13)	0.552(4)	0.39(2)
	P	9.12(42)	17.6(4)	12.7(5)
I_B'	*x* = *y* = *z*	–	0.0752(7)	0.077(1)
	cation	–	Cu	Cu
	frac	–	0.145(7)	0.21(1)
	P	–	4.6(2)	6.6(5)
II	*x* = *y* = *z*	0.2340(1)	0.2465(5)	0.247(1)
	cation	Na	Na	Na
	frac	1.002(14)	0.357(18)	0.18(2)
	P	32.06(45)	11.4(6)	5.8(7)
II′	*x* = *y* = *z*		0.2116(5)	0.2072(5)
	cation		Cu	Cu
	frac		0.162(8)	0.24(1)
	P		5.2(2)	7.8(3)
Al_{efw}	*x* = *y* = *z*			0.037(1)
	cation			Al
	frac			0.24(4)
	P			7(1)
a (Å)		24.79350(7)	24.53029(9)	24.5896(1)

[a] The Si/Al ratio was fixed at 2 in all refinements. Anisotropic temperature factors are indicated by an asterisk (*) and are tabulated in the Supporting Information. The refined extraframework cation temperature factors were 0.044(3), 0.073(4), and 0.072(5) Å^2 for NaY, $Cu^{II}Y$, and $Cu^{I}Y$, respectively. P indicates the number of cations or anions per formula unit. Temperature factors for O(20) and D(21) were constrained to be the same

pattern ($\chi^2 = 7.92$) compared to the Le Bail extraction[41] ($\chi^2 = 1.335$). To locate the copper cation sites, difference Fourier maps were then calculated. Two strong peaks were found initially, and copper cations were inserted at these x x x positions ($x = 0.0508$, I_A', and $x = 0.212$, II′), improving the fit significantly ($\chi^2 = 4.199$). A second Fourier map revealed another x x x site, $x = 0.0761$ (I_B'), with further improvements in the fit ($\chi^2 = 3.63$). The two distinct site I′ cations, A and B, can be resolved in the observed Fourier map (see Supporting Information). Scattering density was also observed on the II site. No cations could be refined at sites I, U, III, IV and V.

The I_B' and II sites are approximately 2.4 Å away from the framework and could therefore be occupied by

(41) LeBail, A.; Duroy, H.; Fourquet, J. L. *Mater. Res. Bull.* **1988**, *23*, 447.

Table 2. Bond Lengths (Å) and Angles (°) for the Zeolite Frameworks in NaY, $Cu^{II}Y$, and $Cu^{I}Y$ from Rietveld Refinements on Data Collected at 298 K

bond/angle	NaY	$Cu^{II}Y$	$Cu^{I}Y$
T−O(1)	1.627(3)	1.624(3)	1.625(4)
T−O(2)	1.656(3)	1.608(3)	1.641(4)
T−O(3)	1.669(3)	1.679(2)	1.661(3)
T−O(4)	1.624(3)	1.610(3)	1.620(3)
mean	1.644(2)	1.63(3)	1.63(1)
T−O(1)−T	138.1(2)	143.9(3)	142.8(3)
T−O(2)−T	145.9(2)	147.6(3)	145.7(3)
T−O(3)−T	139.5(3)	133.8(3)	137.4(3)
T−O(4)−T	149.2(4)	143.8(3)	141.0(4)
mean	143.1(3)	142(5)	141(3)
O(2)−T−O(3)	106.0(2)	102.8(2)	105.4(3)
O(2)−T−O(1)	111.1(2)	110.7(2)	110.7(3)
O(2)−T−O(4)	105.3(2)	110.4(4)	109.7(3)
O(3)−T−O(1)	109.3(2)	109.0(2)	110.0(3)
O(1)−T−O(4)	112.1(2)	112.4(1)	111.6(3)
O(3)−T−O(4)	112.1(2)	111.1(3)	109.3(3)
mean	109.3(2)	109(3)	109(2)

Table 3. Bond Lengths (Å) around the Extraframework Cations in $Cu^{II}Y$ and $Cu^{I}Y$

bond		$Cu^{II}Y$ (Å)	$Cu^{I}Y$ (Å)
$Cu(I_A')$−O(3)	×3	2.079(4)	2.22(1)
$Cu(I_B')$−O(3)	×3	2.53(2)	2.64(3)
$Cu(I_B')$−O(20)	×1	1.92(4)	1.93(4)
O(20)−D(21)	×1	1.09(2)	0.96(3)
Cu(II′)−O(2)	×3	2.219(3)	2.222(5)
Na(II)−O(2)	×3	2.58(1)	2.56(3)
Al_{efw}−O(3)	×3	–	2.126(5)
Al_{efw}−$Cu(I_B')$	×1	–	1.69(1)

Table 4. Bond Angles (°) around the Extraframework Cations in $Cu^{II}Y$ and $Cu^{I}Y$

angle		$Cu^{II}Y$ (°)	$Cu^{I}Y$ (°)
O(3)−$Cu(I_A')$−O(3)	×3	115.6(2)	112.0(8)
O(3)−$Cu(I_B')$−O(3)	×3	88.2(8)	88(1)
O(3)−$Cu(I_B')$−O(20)	×1	118.9(1)	117.1(6)
O(3)−$Cu(I_B')$−O(20)	×1	145.0(1)	143.3(1)
O(3)−$Cu(I_B')$−O(20)	×1	112.6(1)	117.1(6)
$Cu(I_B')$−O(2)−D21	×2	134.9(3)	133.5(4)
O(2)−Cu(II′)−O(2)	×3	119.5(1)	117.28(35)
O(2)−Na(II)−O(2)	×3	95.8(6)	91.1(19)
O(3)−Al_{efw}−O(3)	×3	–	119.7(2)

Table 5. Refinement Statistics for All Rietveld Refinements[a]

	NaY	$Cu^{II}Y$	$Cu^{I}Y$
no. of variables	48	69	63
no. of observables (168°)	3272	3232	3232
R_{WP} (168°)	0.0365	0.0217	0.0171
R_P (168°)	0.0317	0.0191	0.0148
R_{F^*F} (168°)	0.0275	0.0433	0.0360
χ^2 (all histograms)	1.91	1.64	1.45

[a] Agreement indices are quoted for the highest-resolution backscattering data refined for all three samples. For $Cu^{I}Y$ and $Cu^{II}Y$, data from the 90° and low-angle banks were also refined and included in the χ^2 values quoted in the table.

Table 6. Sodium−Oxygen Bond Lengths for NaY at 298 K

		NaY (Å)
Na(I)−O(3)	×6	2.689(3)
Na(I_A')−O(2)	×3	2.941(4)
Na(I_A')−O(3)	×3	2.246(7)
Na(II)−O(2)	×3	2.380(4)
Na(II)−O(4)	×3	2.865(3)

either sodium or a copper cation also bound to another species. This type of multiple site occupancy issue is common in ion-exchanged zeolites and can be resolved by using the analyzed composition together with X-ray diffraction data;[42] it is, however, important to note that the copper-exchanged zeolites here are particularly sensitive to radiation damage, as shown by the refinements in Figure 2. Rietveld analysis of X-ray data recorded for 1 h fit well to the cation distribution derived from neutron diffraction ($\chi^2 = 1.05$, Figure 2a), whereas data collected after 19 h revealed pronounced changes in the intensities of several reflections and no longer matched the neutron-derived model ($\chi^2 = 11.5$, Figure 2b). Significantly, satisfactory refinement of the 19-h dataset (Figure 2c) required occupancy of the III site found in Maxwell and de Boer's study and depopulation of the I_A' site (Table 7). This indicates that the Cu cations rearrange significantly upon exposure to X-rays at room temperature and limits the significance that can be attributed to site occupancy information derived even from the 1-h X-ray dataset. EPR spectroscopy (see Supporting Information) confirms the effect of radiation damage, with the EPR-silent pre-irradiated Cu(I) sample becoming EPR-active ($g = 2.007$) upon exposure to X-rays for 19 h.

Refinement of the $Cu^{II}Y$ 1-h X-ray data set together with the neutron data indicated that the II site is occupied by sodium and the I_B' site solely by copper. The I_B' site is generally occupied by transition metals only when coordinated to extraframework ligands, and inspection of the difference Fourier maps at this stage revealed a site near the center of the sodalite cage that refined to be 2 Å away from the I_B' site. The scattering density on this site was too high to arise purely from oxygen (this requires more than one O per I_B' copper cation), but assuming that this O(20) site is actually positionally disordered O and D from an OD^- unit, there are 4.6(2) I_B' cations and 4.5(1) OD^- bound to them, with chemically sensible distances and angles given in Tables 3 and 4, as discussed later.

Refinement of the positions and occupancies of the extraframework species proceeded smoothly, with all of these species restrained to have the same isotropic displacement parameter. At this stage of the refinement, difference Fourier maps were featureless, and close attention was paid to the aluminosilicate framework. Refinement with anisotropic temperature factors ($\chi^2 = 1.6$) for all framework atoms proved to be clearly superior to an isotropic description ($\chi^2 = 2.3$), particularly for the short-*d*-spacing backscattering histogram (R_F^2 decreased from 9.4 to 5.5% when an anisotropic description was used).

The magnitudes of the displacement ellipsoids for three of the four oxide anions are similar (~0.06 Å^2),

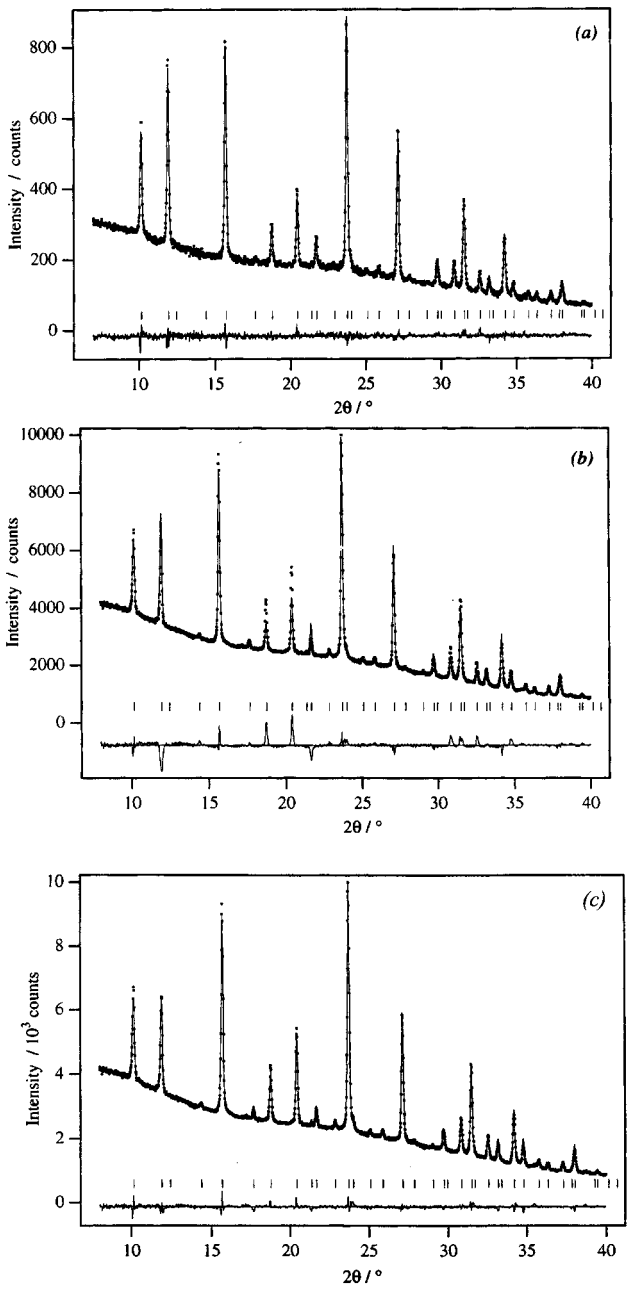

Figure 2. Rietveld refinement fit to Cu Kα powder X-ray data on $Cu^{II}Y$ collected over (a) 1 h (before X-ray damage) and (b) 48 h (after X-ray damage) using the cation distribution derived from neutron diffraction data in both cases. (c) Rietveld fit to the 48h data with the cation distribution given in Table 7.

but the U_{equiv} value of 0.082(1) Å^2 and unusual shape of the ellipsoid indicated that O(2) was behaving in a manner difficult to describe by rigid rotation of the SiO_4 tetrahedra (Figure 3a). The ellipsoid appeared to be elongated in the direction of the Cu(I_A') cation, and resolution of the ellipsoid into components parallel and perpendicular to the O(2)−Cu(I_A') direction revealed an rms displacement of 0.42 Å along this direction [Cu(I_A')−O(2) = 2.878(4) Å]. The I_A' site is located above the centroid of a puckered hexagon of O(3) and O(2) anions, the former providing the three short Cu(I_A')−O(3) distances of 2.079(4) Å that form the primary coordination sphere for this cation. The displacement ellipsoid of O(2) (Figure 4a) suggests that this anion is displaced from its mean position preferentially toward

(42) Wilkinson, A. P.; Cheetham, A. K.; Tang, S. C.; Reppart, W. J. *J. Chem. Soc., Chem. Commun.* **1992**, 1485−1487.

Table 7. Irradiation Damage to $Cu^{II}Y$ as Illustrated from Cation Locations Refined from Powder X-ray Data after a Short Period of Irradiation (1 h) and after Long Irradiation (19 h)

irradiation time		1 h	19 h
Cu (I_A')	$x = y = z$	0.0495(21)	0.0524(6)
	frac	0.480(6)	0.305(9)
	P	15.4(2)	9.8(3)
Cu(I_B')	$x = y = z$	0.09000(53)	0.0849(8)
	frac	0.167(4)	0.238(9)
	P	5.3(1)	7.6(3)
Cu(II′)	$x = y = z$	0.2116(10)	0.1700(13)
	frac	0.137(6)	0.137(5)
	P	4.4(2)	4.4(1)
Na(II)	$x = y = z$	0.2352(8)	0.2299(7) (Cu)
	frac	0.376(19)	0.150(5)
	P	12.0(6)	4.8(1)
Cu(III)	x	–	0.0318(17)
	y	–	0.3870(23)
	z	–	0.0748(15)
	frac		0.033(1)
	P	–	6.3(2)

the I_A' site to provide secondary coordination to this cation, which is otherwise heavily underbonded. This can be interpreted as either a low-energy vibrational mode or a disordered static displacement. In refinements designed to test the latter possibility, it proved possible to refine O(2) at (0.0020, −0.1414, 0.0020) with a split-site model in which 32.8(9)% of the anions occupy an O(2′) position at (0.1254, 0.0093, 0.0093) that is 2.33(2) Å from Cu(I_A'), giving an O(2′)/Cu(I_A') ratio of 1.79(1):1, consistent with the interpretation of the unusual O(2) displacement parameter ellipsoid as arising from secondary bonding to the I_A' copper cation. This displacement produces severe distortion of the tetrahedral angles expected at Si in oxides, with O(2′)−T−O angles of between 83.6(6)° and 127.2(3)°. The mean O−Si−O angle is 109(5)° in the TO_4 units containing O(2′). Although these angles are highly unusual, the resulting refinement is stable and significantly improved over the anisotropic refinement, with $\chi^2 = 1.53$. A more chemically appealing model can be refined by making the O(2′) displaced oxide part of a rigidly rotated TO_4 tetrahedron. This model converges to a similar level of agreement as the anisotropic unsplit framework refinement ($\chi^2 = 1.64$), but because it involves rigid rotation of a fraction of all of the framework oxide anions, it does not address the unique nature of O(2) apparent from the ellipsoids. More seriously, as this rigid rotation involves displacement of O(3) away from I_A' as O(2) approaches it, the primary I_A'−O(3) coordination is thereby weakened. The model tabulated and discussed is therefore the anisotropic unsplit framework model. This model retains chemically sensible T−O−T angles and involves interpretation of the unusual displacement ellipsoid for O(2) as arising from displacements toward Cu(I_A') driven by the need to increase the bonding for this cation with only three oxide anions in its first coordination sphere.

No further features in the difference Fourier maps could be included in the refinement and refined as chemically sensible atomic positions. Attempts to move copper cations away from the 3-fold axis to more general positions were also unsuccessful. The final refined stoichiometry, $Cu_{27.5(1)}(OD)_{4.5(1)}Na_{11.4(2)}Si_{128}Al_{64}O_{384}$, is consistent with the copper cation overexchange indicated by chemical analysis. The copper cation deficit of 5.5 cations per formula unit, compared to the chemical analysis, can be accounted for by unlocated $[CuOD]^+$ groups, possibly in the supercages. Figure 5 shows the observed, calculated, and difference profile plots for all three banks of data collected at 298 K for $Cu^{II}Y$.

(3) $Cu^{I}Y$. The model refined for $Cu^{II}Y$ was used as the starting point for analysis of the $Cu^{I}Y$ data. The framework positions were refined, initially with isotropic displacement parameters, and then the cation positions and their occupancies were refined with the displacement factors fixed and equal to each other. Important differences with respect to the Cu(II) model were apparent in the cation site positions and occupancies, and the unusual framework displacements arising from the O(2) cation were absent. Inspection of the raw data shows a linearly increasing background consistent with the presence of a small amount of adventitious H_2O. Inspection of the difference Fourier map at this stage indicated that there was extra scattering density at the (0.02, 0.02, 0.02) position near the I′ site opposite the double six-ring entrance in the sodalite cage (see Supporting Information) that is not visible in the difference map from the Cu(II) refinement. This is assigned to extraframework Al^{3+} produced by the dealu-

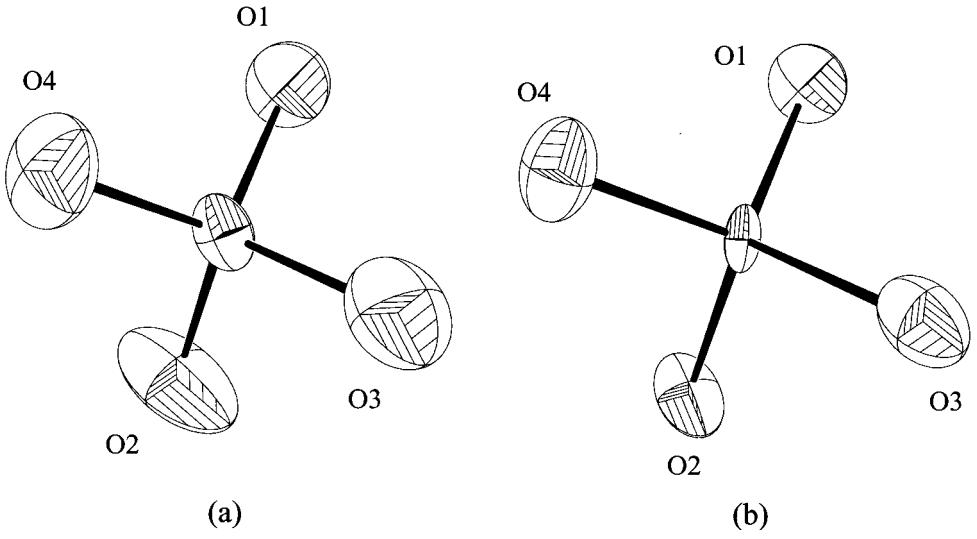

Figure 3. Anisotropic displacement parameters of the TO_4 unit in (a) $Cu^{II}Y$ and (b) $Cu^{I}Y$.

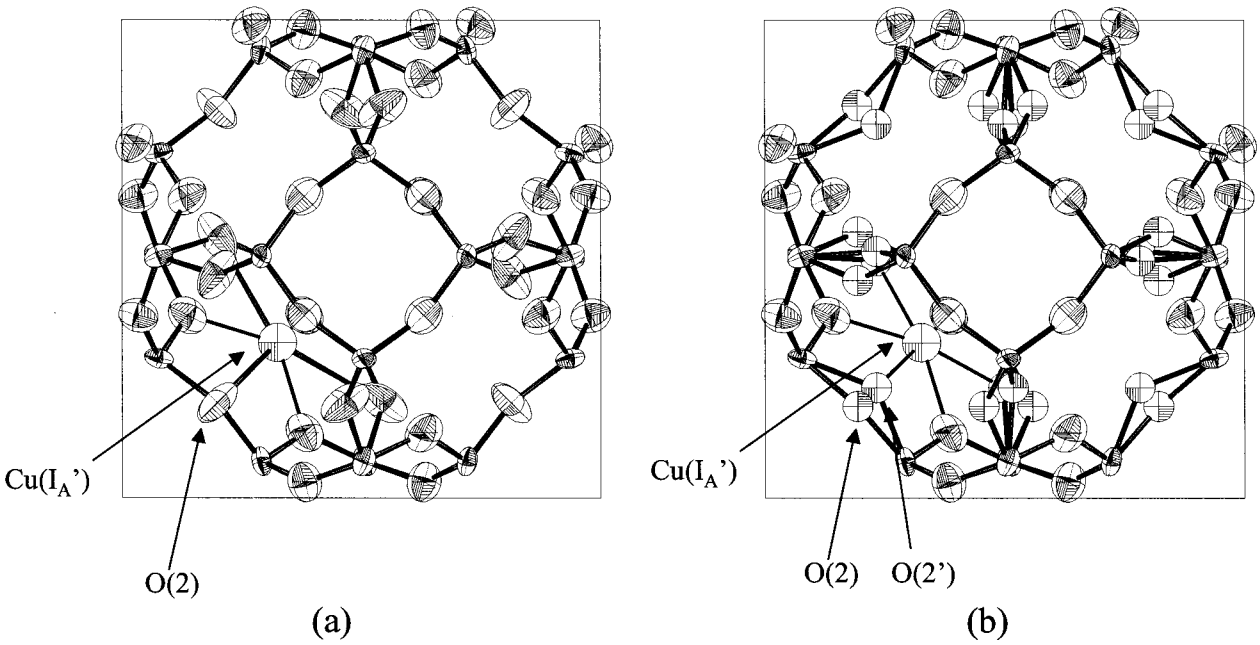

Figure 4. (a) The local displacement of O(2) toward the underbonded Cu(I_A') cation in $Cu^{II}Y$ is shown by the elongation of the O(2) displacement ellipsoid. (b) As in a, showing the split-site model for O(2) in which the O(2′) site represents static displacement of the anion toward the Cu(I_A') cation. Note that, for reasons of clarity, only one Cu atom position is shown in the sodalite cage.

mination (eq 1) invoked to maintain charge balance, and refinement gave 7(1) extraframework Al^{3+} cations occupying this site per unit cell. This site was found to be occupied by aluminum cations after calcination-induced dealumination of LaNaY and CeNaY faujasites.[22] A careful search of the difference map failed to reveal any ordered species bound to the extraframework aluminum. The ($^1/_8$,$^1/_8$,$^1/_8$) location for the AlO_4^- unit in dealuminated HY found by Parise et al.[23] by neutron diffraction was unoccupied in this case.

The extraframework oxygen O(20) site found in the $Cu^{II}Y$ case refined to have zero occupancy in $Cu^{I}Y$, but the difference map revealed excess scattering density near the center of the sodalite cage, and refinement was consistent with 4.6(1) OD units displaced along ⟨111⟩ away from the cage center, 0.35 Å from the EFO site in $Cu^{II}Y$. Despite indications of H contamination from the shape of the background, a search of the negative contours in the difference Fourier map did not reveal any sites that permitted refinement of H. It was therefore assumed that adventitous H_2O was coordinated to cations in the supercage and too positionally or orientationally disordered to contribute to Bragg scattering.

Charge-balance considerations suggest that about 12 protons/deuterons per unit cell should be present in the $Cu^{I}Y$ structure and should most likely be attached to framework oxygen atoms, although if located on a general position, they would only have a fractional occupancy of 0.13 and would thus be difficult to detect. The framework oxide anion temperature factors were refined as isotropic. Deuterons were included in the model at positions as refined by Jirak et al. for HY zeolite.[43] These atoms were heavily constrained to be 1.000(1) Å from the framework oxygen and 2.160(1) Å from the silicon sites. Four deuterons per formula unit could be refined as attached to O(4) under these constraints, but they did not significantly improve the fit, leading to the conclusion that, as in dealuminated HY, there is no crystallographic evidence for ordered protons or deuterons.

As diffraction site occupancies reflect the mean occupancy in an average unit cell, the observation of dealumination implies change to the framework composition, as previous work[24] indicates T-site occupancy remains at 100% as a result of a recrystallization mechanism. On this basis the loss of 7.5 Al^{3+} ions from the T sites gives a new framework composition of $Si_{133}Al_{59}O_{384}^{59-}$, giving a refined composition of $Cu_{27(1)}(OD)_{4.6(2)}Na_{5.8(3)}Si_{133}Al_{59}O_{384}$. In addition to the Cu cation deficit observed for $Cu^{II}Y$, 5.2 sodium cations were not located, possibly bound to adventitious H_2O in the supercage. This difference in H_2O content means that the changes in cation site occupancy cannot be unambiguously attributed to reduction to Cu(I) alone. In the final refinement cycles, all Si/Al and O atoms were refined as anisotropic. This reduced χ^2 from 1.65 to 1.45, a much less significant improvement than in the Cu(II) case. The refinements were not sensitive to the change in Si/Al ratio due to dealumination because of the similar scattering lengths of Si and Al. The refinements are more sensitive to the total T-site occupancy, which refines to 104(1)% and was fixed to 100% in the final refinements, consistent with the recrystallization mechanism. The introduction of seven aluminum T-site vacancies per formula unit to match the level of located extraframework aluminum prevents the refinement of physically acceptable displacement parameters. Refined parameters are given in Table 1, and the observed, calculated, and difference profile plots are shown in Figure 6.

Discussion

The refinements of the Cu(II)- and Cu(I)-containing zeolite Y reveal subtle distinctions in cation site distri-

(43) Jirak, Z.; Vratislav, S.; Bosacek, V. *Phys. Chem. Solids* **1980**, *41*, 1089−1095.

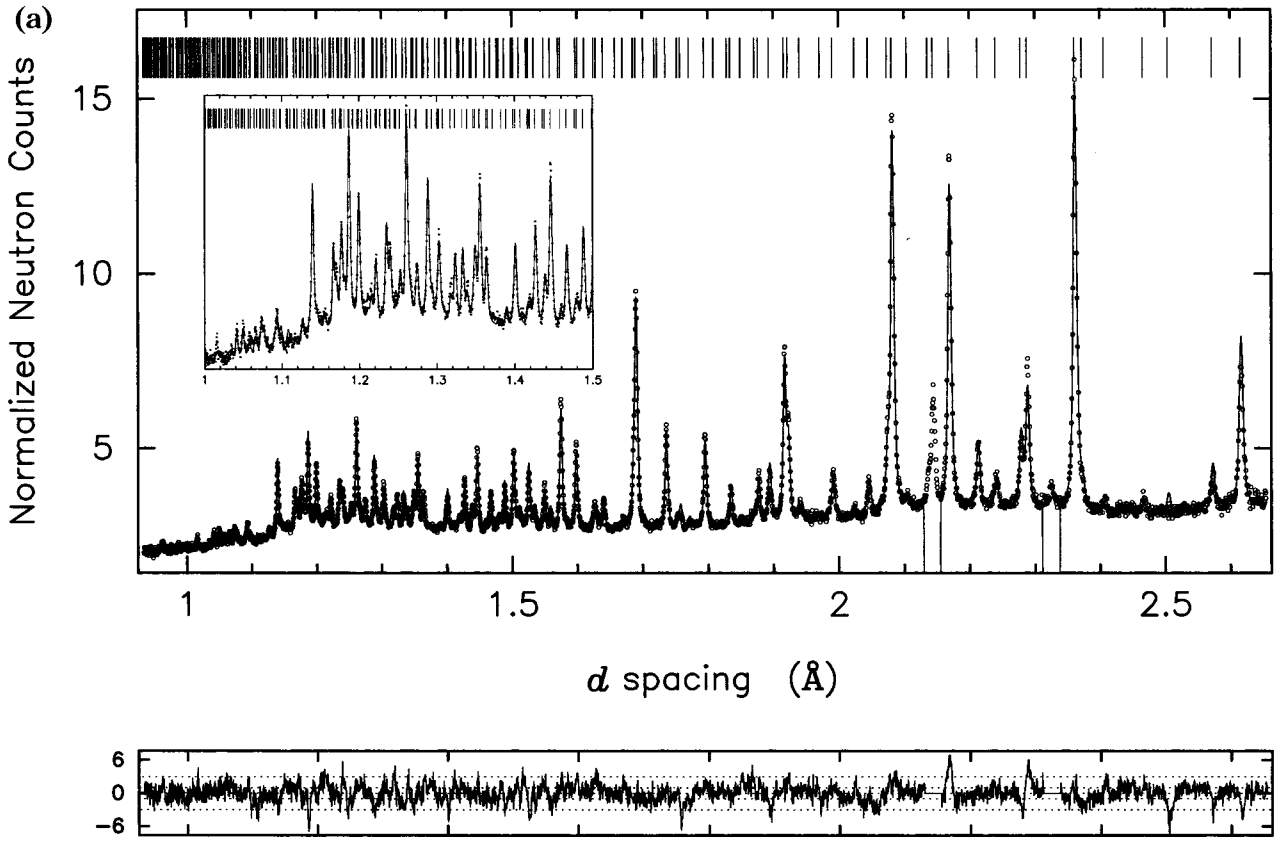
(a)
Normalized Neutron Counts
15
10
5
1
1.5
2
2.5
d spacing (Å)
6
0
−6

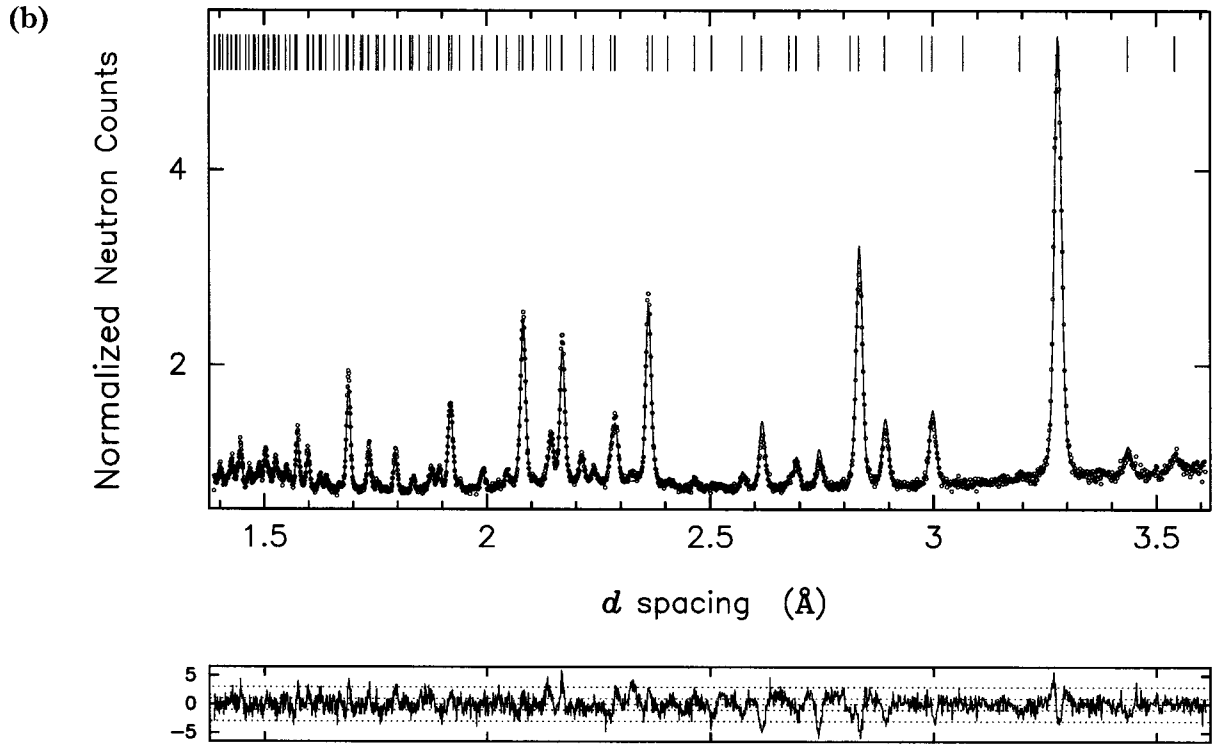
(b)
Normalized Neutron Counts
4
2
1.5
2
2.5
3
3.5
d spacing (Å)
5
0
−5

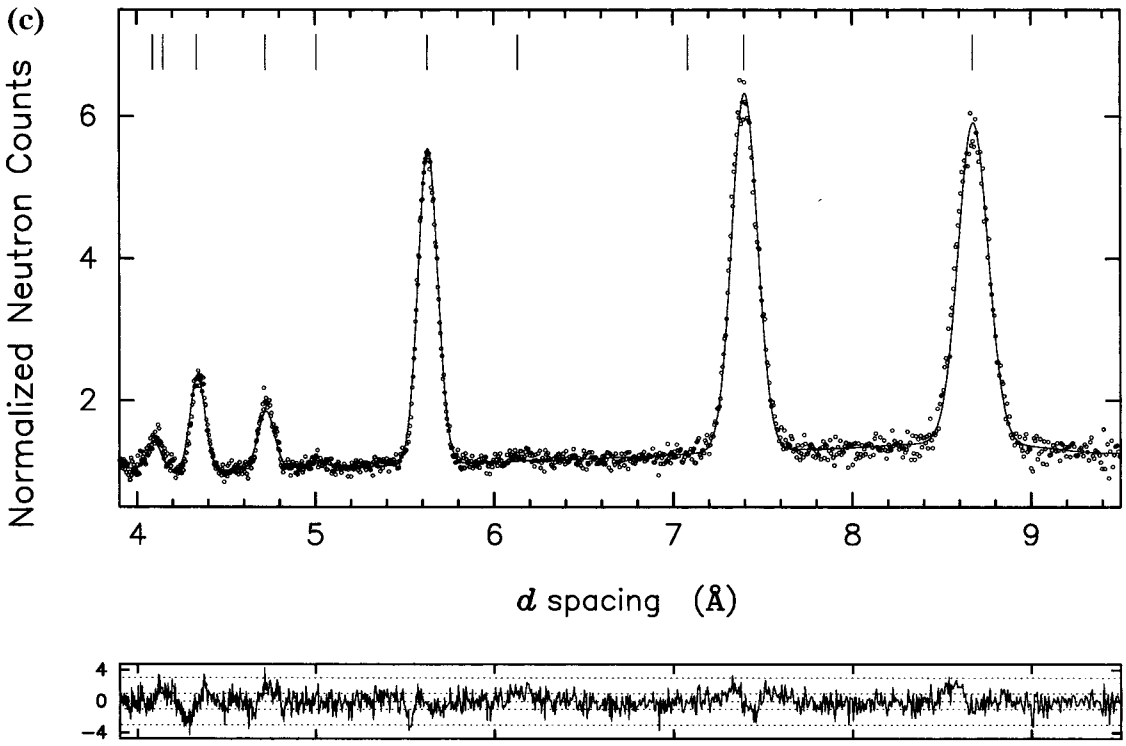

Figure 5. Observed, calculated, and difference powder neutron diffraction profiles for $Cu^{II}Y$ refined from data collected at 298 K on HRPD at (a) backscattering (168°), (b) 90°, and (c) 30°. The observed data are shown as points, the calculated fit is the solid line, and the difference divided by the esd of each point is shown below. Ticks mark the positions of the Bragg reflections. The excluded regions correspond to scattering from the vanadium sample can.

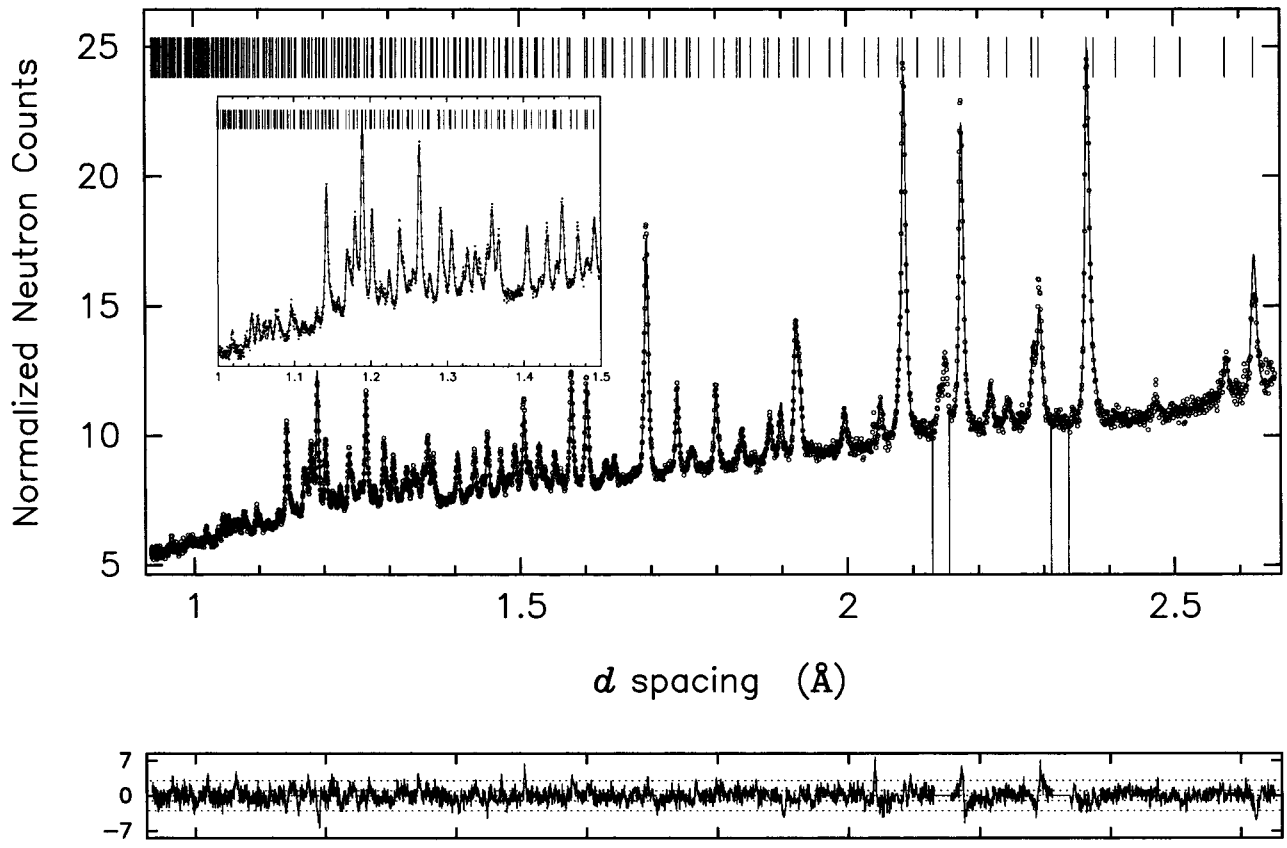

Figure 6. Observed, calculated, and difference powder neutron diffraction profiles for $Cu^{I}Y$ refined from data collected at 298 K on HRPD at backscattering (168°), represented as in Figure 5.

bution (Figure 7) and framework geometry (Figures 3 and 4). Given the complex mechanisms previously invoked to ensure correct charge balancing upon reduction of the Cu(II) to Cu(I) by CO, the most important issue to address arising from the refinements is the matching of framework and extraframework charges:

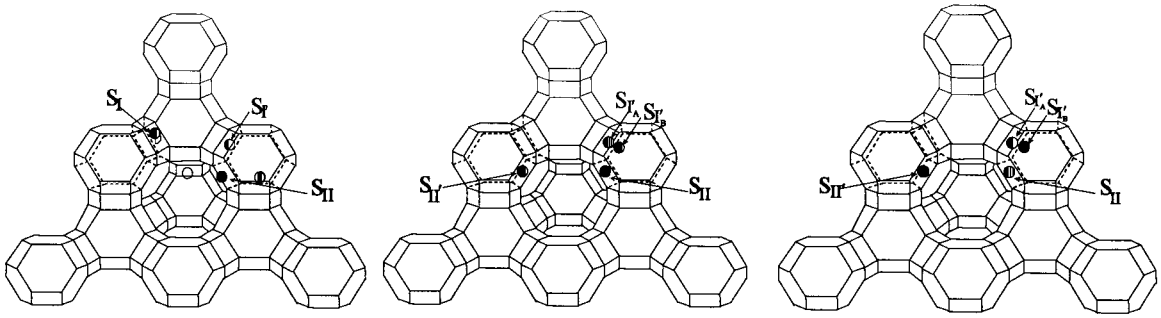

Figure 7. Locations of cations in (a) NaY, (b) $Cu^{II}Y$, and (c) $Cu^{I}Y$. The shading of the spheres indicates the proportion of each site from Figure 1 occupied.

the diffraction data need to be considered together with the bulk analytical data as they are intrinsically insensitive to amorphous or highly disordered regions of the sample. Overexchange of Cu^{II}, resulting from the simultaneous introduction of complexed OD, in the initially prepared $Cu^{II}Y$ and dealumination upon subsequent reduction to $Cu^{I}Y$ are the two limiting charge-compensation mechanisms, and we find evidence for both of them here.

The analyzed $Cu_{33}Na_{12}Si_{130}Al_{62}O_{384}$ composition of $Cu^{II}Y$ demonstrates overexchange and requires 16 extraframework negative charges, of which 4.5(1) are located crystallographically as OD^- in $[Cu(OD)]^+$ groups in the refinement; the remainder can be assigned as bound to the 5.5 unlocated copper cations per formula unit. The site occupancies (discussed in detail later) in $Cu^{II}Y$ give an extraframework charge of 61(2) from the located cations. The $Cu^{I}Y$ refinement provides clear evidence for dealumination, with the extraframework aluminum located at the double six-ring entrance in the sodalite cage: there is no evidence for any ordered extraframework species coordinated to this aluminum site, and consistent with previous crystallographic studies of dealuminated zeolites, the T-site occupancy remains complete. The loss of 7(1) Al^{3+} per cell from the framework requires a new framework composition of $Si_{133}Al_{59}O_{384}$ in $Cu^{I}Y$, with a framework charge of $59(2)^-$. The charge can readily be balanced using the analyzed Na and Cu content of $Cu^{II}Y$ if the extraframework aluminum is counted as contributing +3, but despite the absence of crystallographically located O bound to the extraframework Al^{3+}, it is more conservative to assign these units as $(AlO)^+$ for charge-balancing purposes. The extraframework charge then becomes 49(2), including the 4.5 OD^- groups and the increased number of Cu(I) and Na^+ cations per unit cell due to the framework recrystallization, which is within 3 standard deviations of the minimum-determined (again at the 3σ level) framework charge. This analysis assumes that the crystallographically unlocated EFO invoked in the $Cu^{II}Y$ phase is lost upon reduction to Cu(I). The diffraction data thus demonstrate that dealumination[18] does occur upon reduction to Cu(I), but not to the extent required for complete charge balance, which requires the involvement of extraframework oxygen.[20] Dealumination without reduction in the T-site occupancy requires significant recrystallization of the framework, and the associated reduction in crystallinity that might be expected is indeed evident from the high-resolution diffraction data. The refined values of the Gaussian sigma 1 and Lorentzian gamma 1 profile peak width parameters change from 690(39) and 90(1), respectively, in $Cu^{II}Y$ to 1861(85) and 98(2) to $Cu^{I}Y$, corresponding to full widths at half-maximum of 1705.7 and 4145.9 μs, respectively.

The site occupancies differ from those determined by Maxwell and de Boer, and by Seff,[36] in the absence of cations in the I double six-ring or III sites. It is unusual for a divalent-cation-exchanged zeolite to have site I unoccupied, although this has been unambiguously demonstrated in ZnNaY by resonant X-ray diffraction.[42] In $Cu^{II}Y$, it is primarily the I′ site in the sodalite cage that is occupied by copper cations. There are two distinct Cu environments at 2.079(4) and 2.53(2) Å from three framework oxide anions. The distances at the former I_A' site are close to the expected values for Cu(II)−O distances, although the coordination number of three (Figure 8a) is low. This has consequences for the local structure of the framework, as revealed by the displacement parameters of the TO_4 unit and discussed later. The latter, I_B', is displaced further from the framework by coordination to an OD^- ligand to give a heavily distorted tetrahedral environment (Tables 3 and 4, Figure 8b): the 1.92 Å I_B'−O(20) distance to the coordinating hydroxide compensates for the increased distance from the framework oxide anions, and the 1:1 ratio between the I_B' occupancy and the OD^- concentration confirms that coordination to an extraframework ligand is the driving force for the displacement.

The significant occupancy [5.2(2) cations per cell] of the II′ site (Figure 8c) in the sodalite cage in $Cu^{II}Y$ is an unusual feature and contrasts with the findings of previous work. The II′−O(3) distance of 2.219(3) Å might indicate binding to unlocated extraframework ligands, although the extraframework cation−oxide distances to partly occupied sites are often unphysically long because of averaging between occupied and unoccupied sites. The II′ coordination might therefore actually be trigonal, although considerations similar to those outlined for the I_A' site above apply.

The $Cu^{II}Y$ sample is only partially exchanged for Na^+, and the remaining sodium is located on site II in the supercage, which is the preferred site in NaY itself. The Na^{II}−O(2) distance of 2.58(1) Å is longer than the 2.380(4) Å found for the fully occupied II site in NaY itself as a result of the averaging effect discussed above.

The cation site occupancies in the reduced $Cu^{I}Y$ are slightly but significantly altered from those in the $Cu^{II}Y$ starting material, with the same number of Cu cations located crystallographically in both cases. The occupancies of the I_B' and II′ sites within the sodalite cage

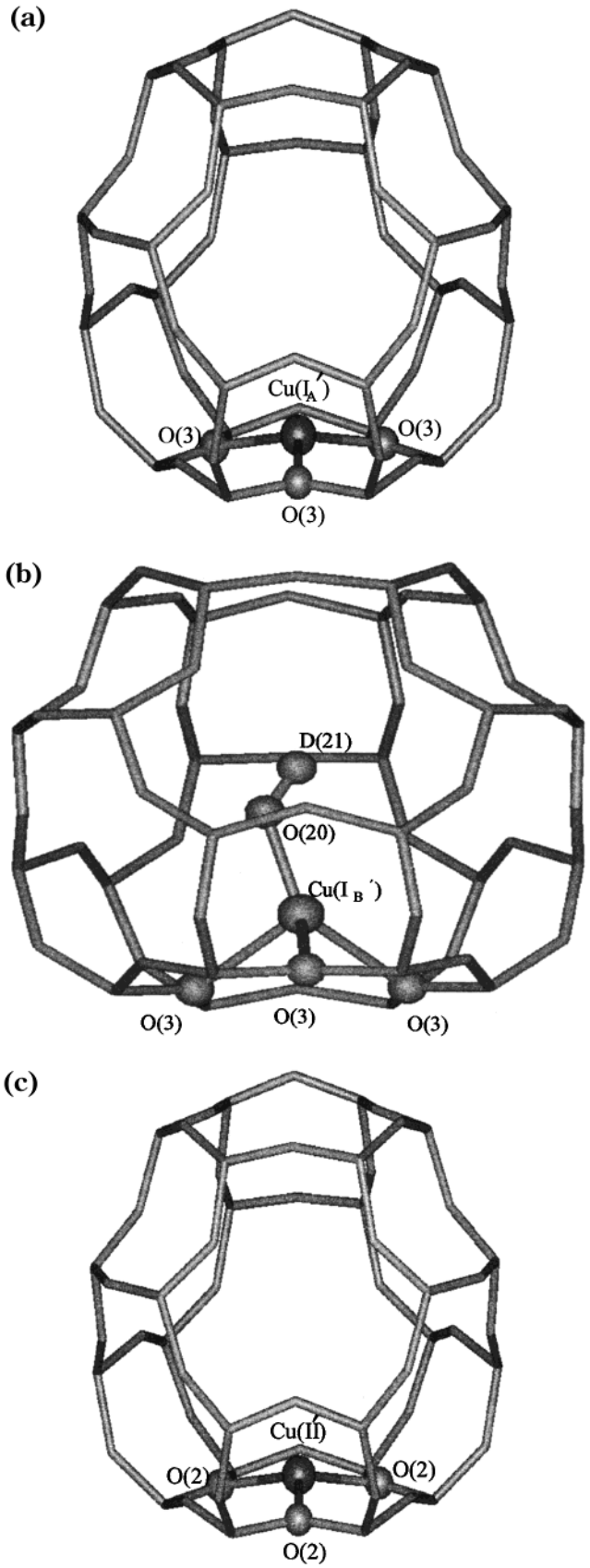

Figure 8. Location and bonding of Cu cations in $Cu^{II}NaY$: (a) site I_A', (b) site I_B', and (c) site II′.

increase, whereas the I_A' occupancy decreases to 66% of its value in $Cu^{II}Y$. The I_A' site is now 2.22(1) Å, rather than 2.079(4) Å, from the coordinating framework oxide, consistent with the larger size of Cu^+. The I_B'−O(4) distance of 2.64(3) Å also increases, although the number of OD^- ions coordinated to this site remains unchanged. The increased scattering density at the I_B' site might therefore also be due to migration of Na^+ cations from the II site (whose occupancy is almost halved in Cu^IY) to the I_B' site, which might be partially occupied by Cu^+ ions coordinated to OD^- and partially by Na^+. The O(3)−Cu(I_B')−O(20) complex has a distorted tetrahedral geometry similar to that found in $Cu^{II}Y$. The II′ site is at similar distances from the framework in both Cu^IY and $Cu^{II}Y$, which is consistent with the loss of crystallographically unlocated extraframework ligands bound to this site in $Cu^{II}Y$ upon reduction to Cu^IY. The II and II′ sites are locally mutually exclusive, and thus the increased II′ occupancy within Cu^IY is correlated with a decreased II occupancy. The redistribution of cations between sites upon reduction might be related to the influence of oxidation state upon catalytic activity.[9]

The extraframework aluminum located close to the framework in the sodalite cage of Cu^IY is a pronounced difference from $Cu^{II}Y$. This might be a further reason for the decreased I′ occupancy by Cu in dealuminated Cu^IY. The Al_{efw}−O(3) distance compares well with that found in dealuminated calcined LaCeY.[22] It is conceivable that some of the enhanced I_B' scattering density is O at a distance of 1.7 Å from Al_{efw}. O(3) has a 0.24 Å rms displacement along the Al_{efw}−O(3) direction, so there might be significant local relaxation of the framework to shorten this Al_{efw}−O(3) bond. Reduction of $Cu^{II}Y$ to Cu^IY produces a 0.24% expansion of the lattice parameters, reflecting both the larger size of Cu^+ and the framework dealumination.

The refinements reveal details of the response of the aluminosilicate framework to reduction of the Cu^{2+} cations: the bond lengths, angles, and displacement parameters all change subtly but significantly. The mean Si/Al−O distances are unchanged between Cu^IY and $Cu^{II}Y$ within error, but the stronger interaction with the Cu(II) ions produces a larger spread of distances in the $Cu^{II}Y$ case. This is related to the observation that the T−O(3) bond is the longest in both cases and that this anion binds to the cation sites that are most highly occupied and closest to the frameworks ($I_A'$and I_B'). The intertetrahedral T−O−T bridging angles also show a larger standard deviation in $Cu^{II}Y$, with the small T−O(3)−T angle being particularly noteable.

The stronger interactions of the Cu^{2+} cations with the aluminosilicate framework result in the larger displacement ellipsoids observed for the framework oxide anions in $Cu^{II}Y$. This is particularly pronounced for O(2), where the ellipsoid is strongly elongated along the O(2)−I_A' direction toward the three-coordinate cation on the I_A' site (Figure 3a). This displacement is interpreted as a local static distortion or low-frequency vibrational mode that reduces the Cu(I_A')−O(2) distance from 2.878(4) to 2.45 Å (Figure 4a). It is possible to identify from difference Fourier maps and subsequently refine a split O(2′) position modeling this displacement, resulting in a 2.28 Å I_A'−O(2′) distance. This does not arise from a rigid rotation of the TO_4 units but represents a local relaxation (which could be static or dynamic) of the framework. It reflects the preference of Cu^{2+} for coordination numbers higher than three: this relaxation of

O(2) produces three secondary coordination contacts between oxide ions and the I_A' copper cation. Cu^+ is generally more stable in lower-coordination-number environments than Cu^{2+}, and therefore, the 3-fold coordination at the I_A' site does not induce similar relaxation of the O(2) cation in Cu^IY. The present data do not permit a chemically sensible refinement of the static locally displaced structure around the Cu^{2+} sites, but the more pronounced, and directional, displacements in the Cu^{2+} phase indicate that the need to increase the copper coordination environment beyond three has a strong effect on the framework. Copper cations show a number of different coordination environments in various zeolites. Single-crystal X-ray diffraction data on Cu-A has been refined for a number of different crystals subjected to different heat treatments.[44] The different crystals show different hydration levels and cation oxidation states. For example, in a crystal desolvated at 350 °C, there are five Cu(II) cations located in the planes of the six-oxygen rings. These ions are each coordinated to three framework oxygen atoms at a distance of 2.11(1) Å. One trigonally coordinated Cu(I) cation is again reported, but this time, it is some 1.27 Å into the cavity. In addition there is a $Cu^+-OH^--Cu^+$ group located well away from the framework.

In partially dehydrated copper mordenite,[1] there are three copper sites, with long Cu−O bonds of between 2.59 and 2.875 Å. The low coordination and high accessibility of the two cation sites in the partially dehydrated zeolite are thought to provide a possible explanation for the high activity of mordenite for the decomposition of nitrogen oxide. In copper ferrierite, another zeolite that is active and selective for nitric oxide decomposition, the copper cations are located on one site only and have two short bonds to the framework oxygen atoms of 2.03(3) and 2.21(3) Å. In CuY, the Cu^{2+} cations are all located in the sodalite cage with its narrow six-ring windows, which might hinder access to gaseous reagents in potential catalytic deNO_x reactions. The mobility of these cations in the presence of ligands should not be neglected however.

The site occupancies derived from analysis of the powder X-ray data differ markedly depending on the data collection time, reflecting the dramatic changes in X-ray pattern with time in the beam. This radiation sensitivity is particularly marked for Cu^IY. Radiation damage of dehydrated MnNaY,[45] CaY, and LaY[46] has been observed previously and shown to produce cation redistribution. EPR evidence is consistent with the formation of superoxide centers. In CuY, it is the (111) and (200) reflections that change most upon irradiation, and it might be significant that these data were excluded from previous X-ray refinements. Refinement of the radiation-damaged $Cu^{II}Y$ (Table 7) leads to depopulation of the I_A' site, with the cations displaced from this site occupying the previously unpopulated III site.

Conclusion

Neutron powder diffraction has revealed the subtle changes in cation site occupancy and cation framework interaction that are associated with reduction of $Cu^{II}Y$ to Cu^IY. The role of both dealumination and extraframework oxygen introduced during ion exchange has been demonstrated. The larger Cu(I) cation exerts a much reduced distorting effect on the aluminosilicate framework, whereas the unfavorable three-coordination of Cu(II) induces framework relaxation evident from the atomic displacement parameters.

Acknowledgment. We thank EPSRC and CCLRC for a CASE studentship for A.J.F. and for funding for the beam time. We thank Professor R. Townsend and Dr. M. Webb of Unilever for the NaY.

Supporting Information Available: Anisotropic displacement parameters for $Cu^{II}Y$, Cu^IY, and NaY. Neutron powder diffraction profiles for NaY refined from data collected on HRPD at 298 K at backscattering (168°), 90°, and 30°. Neutron powder diffraction profiles for Cu^IY refined from data collected on HRPD at 298 K at 90° and 30°. Observed Fourier map showing sites I_A' and I_B' in Cu^IY. EPR data on Cu(I) before and after X-ray irradiation. Difference Fourier map for Cu^IY showing density assigned as extraframework aluminum in the sodalite cage. This material is available free of charge via the Internet at http://pubs.acs.org.

CM010504B

(44) Lee, H. S.; Seff, K. *J. Phys. Chem.* **1981**, *85*, 397−405.

(45) Pearce, J. R.; Mortier, W. J.; Uytterhoeven, J. B. *J. Chem. Soc., Faraday Trans. I* **1979**, *75*, 898−906.

(46) Costenoble, M. L.; Mortier, W. J.; Uytterhoeven, J. B. *J. Chem. Soc., Faraday Trans. I* **1978**, *74*, 477−483.